Cite this: *Phys. Chem. Chem. Phys.*, 2012, **14**, 6898–6904

www.rsc.org/pccp

PAPER

Mechanistic aspects of photo-induced formation of peroxide ions on the surface of cubic Ln_2O_3 (Ln = Nd, Sm, Gd) under oxygen†

Xiao-Lian Jing, Qing-Chuan Chen, Chong He, Xue-Quan Zhu, Wei-Zheng Weng,* Wen-Sheng Xia and Hui-Lin Wan*

Received 10th January 2012, Accepted 20th March 2012
DOI: 10.1039/c2cp40086c

The photo-induced formation of peroxide ions on the surface of cubic Ln_2O_3 (Ln = Nd, Sm, Gd) was studied by *in situ* microprobe Raman spectroscopy using a 325 nm laser as excitation source. It was found that the Raman bands of peroxide ions at 833–843 cm^{-1} began to grow at the expense of the Ln^{3+}–O^{2-} bands at 333–359 cm^{-1} when the Ln_2O_3 samples under O_2 were continuously irradiated with a focused 325 nm laser beam at temperatures between 25–150 °C. The intensity of the peroxide Raman band was found to increase with increasing O_2 partial pressure, whereas no peroxide band was detected on the Ln_2O_3 under N_2 as well as on the samples first irradiated with laser under Ar or N_2 followed by exposure to O_2 in the dark. The experiments using ^{18}O as a tracer further confirmed that the peroxide ions are generated by a photo-induced reaction between O_2 and the lattice oxygen (O^{2-}) species in Ln_2O_3. Under the excitation of 325 nm UV light, the transformation of O_2 to peroxide ions on the surface of the above lanthanide sesquioxides can even take place at room temperature. Basicity of the lattice oxygen species on Ln_2O_3 also has an impact on the peroxide formation. Higher temperature or laser irradiation power is required to initiate the reaction between O_2 and O^{2-} species of weaker basicity.

1. Introduction

The selective oxidation process plays an important role in the modern petrochemical industry.[1] Molecular oxygen has the advantage over other oxidants for the selective oxidation reaction in that it is inexpensive and environmentally friendly.[2] As the energy barrier for electron transfer from the organic substrate to O_2 is usually high for the uncatalyzed oxidation reaction, the activation of molecular oxygen to form the active oxygen species is usually required before O_2 can participate in the reaction as oxidizing agent.[3,4] Understanding the activated forms of oxygen species in the reaction as well as the pathways by which molecular oxygen becomes activated on the catalyst is therefore of fundamental importance in oxidation catalysis.[3–6] Due to their excellent chemical and thermal stabilities and electronic characteristics, lanthanide oxides have been widely used as catalysts in the catalytic oxidation of light alkanes such as oxidative coupling of methane (OCM) and oxidative dehydrogenation of ethane (ODE).[7–14] It is well-documented that OCM catalysts with stable cationic valence such as La_2O_3 can only be used in cofeed operation and show practically no activity with methane in the absence of O_2.[14–18] These results indicated that certain active oxygen species generated by interaction of molecular oxygen with the oxide catalysts were required to initiate the reaction. The results of isotopic labeling experiments suggest that the active oxygen species is formed by dissociative adsorption of molecular oxygen over the La_2O_3 surface.[19–21] The results of periodic density functional theory calculations also indicated that surface oxygen species such as peroxide (O_2^{2-}) ions could be generated by adsorption of O_2 molecules at surface oxygen vacancies, followed by dissociative adsorption of O_2 across the closed-shell oxide surface of La_2O_3 (001).[22] A number of spectroscopic investigations have centered around the nature of the active oxygen species for the OCM reaction over rare earth oxide catalysts. Mestl *et al.* reported the presence of a Raman band characteristic of O_2^{2-} on the surface of La_2O_3 catalysts at 700 °C under O_2 and $CH_4/O_2/He$ = 4/1/8 atmospheres.[23] Besides, the superoxide O_2^- has also been proposed to be the active oxygen species for the OCM reaction based on the results of *in situ* Raman characterization over rare earth oxide based catalysts under the OCM condition.[24]

State Key Laboratory of Physical Chemistry of Solid Surfaces, National Engineering Laboratory for Green Chemical Productions of Alcohols, Ethers and Esters, Department of Chemistry, College of Chemistry and Chemical Engineering, Xiamen University, Xiamen 361005, China. E-mail: wzweng@xmu.edu.cn, hlwan@xmu.edu.cn; Fax: (+86)592-2185192; Tel: (+86)592-2186569

† Electronic supplementary information (ESI) available: XRD patterns of cubic Ln_2O_3 (Ln = Nd, Sm, Gd), the additional Raman information for the photooxygenated Gd_2O_3 and Nd_2O_3 samples and the details on the calculation of band positions for the peroxide ions. See DOI: 10.1039/c2cp40086c

During a study on the La_2O_3 under O_2 by microprobe laser Raman spectroscopy, we discovered that the laser not only acts as an excitation source for Raman scattering but also induced the formation of lanthanide peroxide linkages (La^{3+}–O_2^{2-}) on the La_2O_3 surface.[25] This observation indicates that Raman results may be complicated by an artifact arising from laser excitation. It also raises questions about the photochemistry of lanthanide oxide surfaces under oxygen. As a continuation of the previous research, a more extensive *in situ* Raman investigation aiming at understanding the mechanistic details of the photo-induced formation of peroxide ions on the surface of lanthanide sesquioxides is presented in this paper. Roles of molecular oxygen and lattice oxygen species of lanthanide sesquioxide in the peroxide formation were investigated by performing the experiments under different O_2 partial pressures as well as using ^{18}O as a tracer. The effects of temperature, laser irradiation power and the basicity of Ln_2O_3 on the formation of peroxide ions over three cubic Ln_2O_3 (Ln = Nd, Sm, Gd) samples were systematically studied. Based on these results, a mechanism for the photo-induced formation of peroxide ions on the surface of lanthanide sesquioxides was proposed. The thermal stability of the peroxide ions formed on different lanthanide sesquioxides was also compared.

2. Experimental section

2.1 Sample preparation

Preparation of cubic Nd_2O_3: Cubic Nd_2O_3 was prepared form $Nd(OH)_3$ according to relevant references.[26,27] First, a commercial Nd_2O_3 (99.99%; Alfa Aesar) sample was treated at 100 °C for 100 h with a 21% O_2/N_2 flow containing water vapor (by bubbling 21% O_2/N_2 through H_2O at room temperature) to form $Nd(OH)_3$. $Nd(OH)_3$ was then heated at 650 °C in a flow of 21% O_2/N_2 (50 mL min^{-1}) for 3 h to get cubic Nd_2O_3.

Preparation of cubic Sm_2O_3 and Gd_2O_3: A commercial Ln_2O_3 (Ln = Sm and Gd; Alfa Aesar, 99.99%) sample (0.005 mol, *e.g.* Gd_2O_3, 1.81 g) was dissolved in an excess amount of concentrated nitric acid (65%, A.R.). The solution was then heated at 110 °C for 24 h to remove H_2O and the excess amount of nitric acid to form $Ln(NO_3)_3$. The solid product was then dissolved in 30 mL deionized water. After that, the $Ln(NO_3)_3$ solution was added slowly under vigorous stirring into a mixture of $NH_3{\cdot}H_2O$ (3.0 mL; 25%, A.R.) and H_2O_2 (16.5 mL; 30 wt%, A.R.) kept at 0 °C in an ice-water bath. The mole ratio of $Ln^{3+}:H_2O_2:NH_3{\cdot}H_2O$ is about 1 : 16 : 4. After 2 h stirring in the ice-water bath, the precipitate was isolated by centrifugation (rotation speed 3600 r min^{-1}). The solid product was dried at 110 °C for 24 h and calcined at 650 °C in a flow of 21% O_2/N_2 (50 mL min^{-1}) for 3 h.

The BET surface areas of Nd_2O_3, Sm_2O_3 and Gd_2O_3 are 6.9, 39.4 and 48.3 $m^2\ g^{-1}$, respectively. The data were measured by N_2 adsorption at −196 °C with a Micromeritics TriStar II 3020 instrument. Before the measurements, the samples were degassed at 200 °C for 3 h.

2.2 XRD characterization

X-ray powder diffraction (XRD) analysis was carried out at room temperature with a Panalytical X'pert PRO diffractometer. Cu-Kα radiation obtained at 40 kV and 30 mA was used as the X-ray source.

2.3 Raman spectroscopic characterization

The Raman spectra were recorded on a Renishaw R1000 microprobe Raman system equipped with a CCD detector using a 325 nm He-Cd laser as the excitation source. The microscope attachment for the spectrometer is based on a Leica DMLM system with an OFR LMU-15×-NUV objective. Spectra acquisition time was varied for different experiments and 50 s was the most commonly used one. The laser spot on the sample is about 3 μm in diameter and the spectral resolution is about 6 cm^{-1}. The maximum laser power of the spectrometer measured at the analysis spots is 3–4 mW. In some experiments, lower laser power (*e.g.* 0.3–0.4 mW) was used in order to minimize the effect of laser irradiation during spectrum recording.

In all experiments, a Ln_2O_3 sample was first heated under flowing O_2 (99.995%; Linde) at 650 °C for 180–360 min to remove carbonates and moisture. The sample was then cooled in the dark to a specified temperature under O_2 before it was exposed to a focused 325 nm laser beam of the Raman spectrometer to induce formation of peroxide ions and record the spectra. The flowing rate of O_2 over samples was ~50 mL min^{-1}.

The ^{18}O-labelled Nd_2O_3 was obtained by treating a normal cubic Nd_2O_3 sample with a flow of $^{18}O_2$ (97%; CIL) at 650 °C for 6 h. The sample was then cooled in the dark under $^{18}O_2$ to room temperature and exposed to a focused 325 nm laser beam of the Raman spectrometer to induce formation of peroxide ions and record the spectra. The flowing rate of $^{18}O_2$ over the sample was ~5 mL min^{-1}.

The Raman spectra of pure Ln_2O_3 samples were recorded under N_2 at room temperature. Before recording the spectra, the samples were heating at 650 °C under flowing N_2 (99.999%; Linde) for more than 180 min. The flowing rate of N_2 over the samples was ~50 mL min^{-1}.

2.4 CO_2-TPD experiment

The CO_2-temperature-programmed desorption (CO_2-TPD) experiments were performed with a MS-TPD apparatus. The fresh Ln_2O_3 (1.0 g) was first treated in a flow of He (99.999%, Linde; 20 mL min^{-1}) at 650 °C for 60 min to remove carbonates and moisture. The sample was then cooled to 20 °C and treated with a flow of CO_2 (99.995%, Linde; 20 mL min^{-1}) for 60 min, followed by purging with He for about 30 min until the baseline was flat. The TPD profile was obtained by heating the CO_2 pre-treated sample from 20 to 900 °C at a rate of 10 °C min^{-1} in a flow of He (20 mL min^{-1}). The effluent gas mixture was passed through a cold trap at ~−60 °C to remove water before it was analyzed by an on-line mass spectrometer (Hiden QIC-20). Ions at 44 (CO_2) m/z value were detected during on-line measurements.

3. Results and discussion

3.1 Photo-induced formation of peroxide ions on the surface of cubic Ln_2O_3 (Ln = Nd, Sm, Nd) under oxygen

The Raman spectra reported below were obtained in a home built high temperature *in situ* Raman cell specially designed for

the spectrometer. A diagram of this Raman cell is available elsewhere.[28] The laser (325 nm) of the Raman spectrometer was also used to induce formation of peroxide ions on the samples. Raman spectra (Fig. 1 insets) of cubic Ln_2O_3 (Ln = Nd, Sm, Gd) presented in this work are in good agreement with the literature.[29–32] All of them are characterized by the presence of a very strong band in the range between 336–359 cm^{-1} which can be assigned to a combination of A_g mode and F_g mode of metal–oxygen vibrations.[32–34] The structure of samples was further confirmed by the results of XRD analysis (Fig. S1 in the ESI†). When the Nd_2O_3, Sm_2O_3 and Gd_2O_3 samples under oxygen were continuously irradiated with a focused 325 nm laser beam (~3 μm in diameter) of the Raman spectrometer at 25, 100 or 150 °C, Raman bands at 833–843 cm^{-1}, which represent the O–O stretching mode (ν_{O-O}) of a peroxide species,[35–37] began to grow at the expense of the Ln^{3+}–O^{2-} bands at 333–359 cm^{-1} (Fig. 1). After being irradiated with the laser at 150 °C for 120 min, the intensity of the peroxide band on the Gd_2O_3 was found to be attenuated with increasing distance from the center of the laser beam, and became almost zero at ~120 μm (Fig. S2 in the ESI†). This result clearly demonstrates that it is the laser irradiation not the thermal heating that causes the formation of peroxide species. Fig. 2 shows Raman spectra recorded on cubic Nd_2O_3 and Gd_2O_3 after the samples under N_2, 11% O_2/N_2 and O_2 were continuously irradiated with a focused 325 nm laser beam for 30 or 60 min. It can be seen that the intensities of the peroxide Raman band on the samples increased with increasing O_2 partial pressure, and no peroxide band was detected on the Ln_2O_3 under N_2. This result indicates that molecular oxygen is required in the formation of peroxide ions. The subsequent experiments also confirmed that no Raman band at ~840 cm^{-1} was found on the Ln_2O_3 sample, which was first irradiated with laser under N_2 or Ar followed by exposure to O_2 in the dark. These observations indicated that the peroxide ions detected on the samples after laser irradiation should have resulted from a photo-induced transformation (or activation) of O_2 molecules on the surface of Ln_2O_3.

Generally speaking, activation of molecular oxygen on metal or oxide catalyst occurs in a stepwise manner according

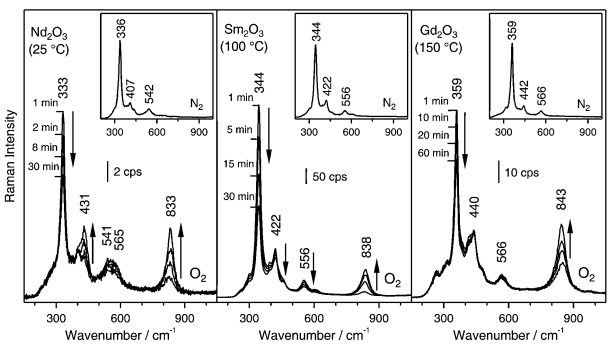

Fig. 1 *In situ* Raman spectra of the cubic Ln_2O_3 (Ln = Nd, Sm, Gd) continuously irradiated with a focused 325 nm laser beam under O_2 in a microprobe Raman spectrometer at indicated temperatures for 30 or 60 min. The laser powers used to induce the formation of peroxide species on Nd_2O_3, Sm_2O_3 and Gd_2O_3 samples were 0.4, 0.75 and 2.1 mW, respectively. Inset: the Raman spectra of cubic Ln_2O_3 (Ln = Nd, Sm, Gd) recorded under N_2 atmosphere at 25 °C.

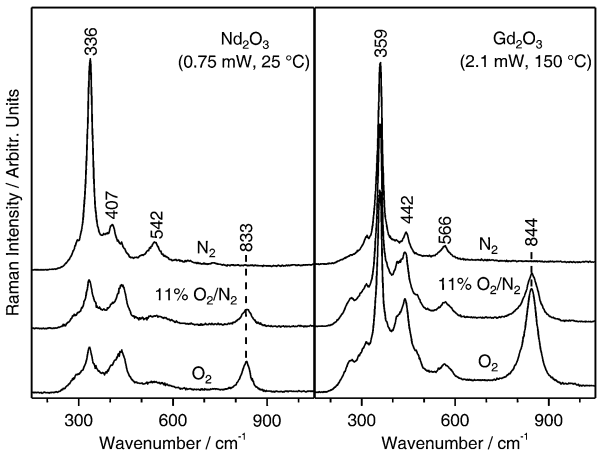

Fig. 2 The effect of O_2 partial pressure on the intensity of the peroxide Raman band formed on cubic Ln_2O_3 (Ln = Nd and Gd). The spectra were recorded after the samples under N_2, 11% O_2/N_2 and O_2 atmospheres were continuously irradiated with a focused 325 nm laser beam for 30 (Nd_2O_3) and 60 (Gd_2O_3) min. The temperatures and laser irradiation powers used to induce the formation of peroxide species as well as to record the spectra are indicated in the figures.

to the scheme (eqn (1)) proposed by Kazanskii *et al.*[38,39] in which O_2 adspecies ($\underline{O}_2$) accept electrons from the catalyst and are gradually transformed to a series of negatively charged oxygen species of either electrophilic ($\underline{O}_2^-$, $\underline{O}_2^{2-}$, $\underline{O}^-$) or nucleophilic ($\underline{O}^{2-}$) nature.[3,40]

$$O_{2(g)} \longrightarrow \underline{O}_2 \xrightarrow{e} \underline{O}_2^- \xrightarrow{e} \underline{O}_2^{2-} \longleftrightarrow 2\underline{O}^- \xrightarrow{2e} 2\underline{O}^{2-} \quad (1)$$

As can be seen from eqn (1), the transformation of O_2 on the surface of Ln_2O_3 to a peroxide ion required two electrons from the oxide to reduce the O_2 adspecies. In any metal oxide sample with stable cationic valence, electrons for reducing an O_2 molecule may come from either lattice oxygen ions (O^{2-}) or surface F centers (an oxygen vacancy which has captured two elections[19,41]). However, in consideration of the facts that the amount of F centers in oxide is very limited and that the development of the Raman band for peroxide at 833–843 cm^{-1} is accompanied by a decline of the band for Ln^{3+}–O^{2-} at 336–359 cm^{-1} (Fig. 1), it is rational to conclude that the electrons for the reduction of an O_2 molecule mainly come from the lattice oxygen species on the Ln_2O_3 surface.

As we all know that an O_2 molecule in the ground state is an open shell triplet $^3\Sigma_g^-$, whereas the peroxide species is in the singlet state. If the triplet ground state O_2 molecule adsorbs and dissociates on the Ln_2O_3 surface following the mechanisms suggested by Palmer *et al.* based on the results of periodic density functional theory calculations,[22] leading to the formation of surface peroxide species, there should exist a spin-state flipping from the triplet potential energy surface to the singlet potential energy surface to satisfy the requirement of the spin conservation rule. Recently, Lu *et al.* carried out a density functional theory study of molecular oxygen adsorptions on the BaO (100) surface.[42] The results show that the triplet ground state O_2 molecule first binds electrostatically on top of the surface Ba^{2+} site. It further quenches to the singlet potential energy surface to form a covalently bonded O_3^{2-} species, which acts as the key precursor for further dissociation, leading

eventually to the formation of surface peroxides O_2^{2-}. The replacement of the Ln^{3+}–O^{2-} band by the peroxide band as demonstrated in Fig. 1 can therefore be regarded as a photo-induced oxygenation of the lattice oxygen species on the Ln_2O_3 micro crystal surface by molecular oxygen, in which UV excitation provides the necessary energy for the transformation of triplet O_2 to the singlet state to satisfy the requirement of the spin conservation rule.[25] The participation of O^{2-} in the formation of peroxide was further confirmed by the experiment performed with a cubic Nd_2O_3 sample partially labelled with ^{18}O. As shown in Fig. 3, cubic $Nd_2{}^{16}O_3$ is characterized by an intense band at 336 cm^{-1} for the Nd^{3+}–$^{16}O^{2-}$ vibration (Fig. 3a). After a $Nd_2{}^{16}O_3$ sample was treated with a flow of $^{18}O_2$ at 650 °C for 6 h followed by cooling under $^{18}O_2$ to room temperature, the Nd^{3+}–O^{2-} vibration band shifted from 336 to 320 cm^{-1} (Fig. 3b). The latter is very close to the band position of Nd^{3+}–$^{18}O^{2-}$ (319 cm^{-1}) calculated based on the wavenumber of Nd^{3+}–$^{16}O^{2-}$ at 336 cm^{-1} by assuming a simple harmonic oscillator model, indicating that almost all of the $^{16}O^{2-}$ atoms on the Nd_2O_3 micro crystal surface (at least those within the detection depth of Raman spectroscopy) were replaced by $^{18}O^{2-}$. Irradiation of the ^{18}O-labelled Nd_2O_3 under $^{18}O_2$ flow with a 0.3 mW of 325 nm laser beam at 25 °C for 15 min revealed a band at 790 cm^{-1} (Fig. 3c). When the laser power was raised to 0.75 mW, a shoulder band at 811 cm^{-1} appeared (Fig. 3d). The latter became noticeable after the laser power was increased to 3.0 mW (Fig. 3e). A simple calculation based on the diatomic harmonic oscillator model using the ν_{O-O} band of $^{16}O_2^{2-}$ at 833 cm^{-1} gave band positions at 786 and 810 cm^{-1} for the $^{18}O_2^{2-}$ and $(^{18}O^{16}O)^{2-}$ peroxide ions, respectively (the details on the calculation of band positions for the $^{18}O_2^{2-}$ and $(^{18}O^{16}O)^{2-}$ peroxide ions are given in the ESI†). The calculated band positions were in quite reasonable agreement with the experimental results shown in Fig. 3 when factors such as the anharmonicity and the width of the band were taken into account.[43] These results indicated that when the ^{18}O-labelled Nd_2O_3 sample under $^{18}O_2$ flow was exposure to a 325 nm laser beam of relatively low power (*e.g.* 0.3 mW)

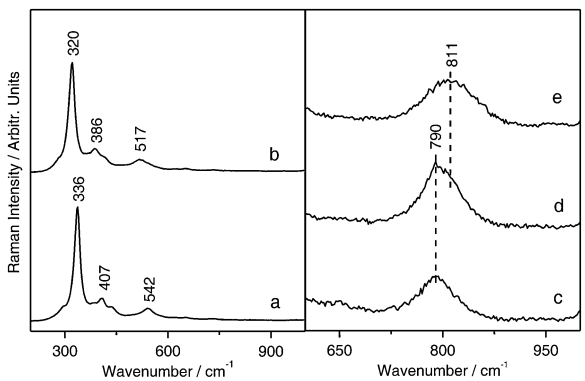

Fig. 3 Raman spectra of (a) normal cubic Nd_2O_3, (b) ^{18}O-labelled cubic Nd_2O_3 and the peroxide ions formed on ^{18}O-labelled cubic Nd_2O_3 after the sample under $^{18}O_2$ was continuously irradiated with a focused 325 nm laser beam of (c) 0.3 mW, (d) 0.75 mW and (e) 3.0 mW at 25 °C for 15 min. The laser power used to record the spectra was 0.3 mW. All the spectra were recorded at 25 °C.

at 25 °C, $^{18}O^{2-}$ species on the surface of the Nd_2O_3 micro crystals first reacted with $^{18}O_2$, leading to the formation of $^{18}O_2^{2-}$ peroxide ions (790 cm^{-1}) (Fig. 3c). With the increasing of the laser irradiation power to 0.75 mW, both $^{18}O_2^{2-}$ and $(^{18}O^{16}O)^{2-}$ peroxide ions were formed (Fig. 3d). Obviously, ^{16}O in the peroxide ions can only come from the ^{18}O-labelled Nd_2O_3 which was prepared by treating $Nd_2{}^{16}O_3$ with $^{18}O_2$. The observation of the $(^{18}O^{16}O)^{2-}$ peroxide Raman band indicated that even though the $Nd_2{}^{16}O_3$ sample had been treated with $^{18}O_2$ at 650 °C for 6 h, the $^{16}O^{2-}$ species in the bulk phase of Nd_2O_3 micro crystals were still not fully replaced by $^{18}O^{2-}$. The above result also indicated that $^{16}O^{2-}$ species in the bulk of the Nd_2O_3 micro crystals were involved in the formation of peroxide ions. The $(^{18}O^{16}O)^{2-}$ peroxide ions could have resulted from diffusion of the $^{16}O^{2-}$ species in the bulk phase of Nd_2O_3 micro crystals to the surface layer followed by isotopic exchange with the $^{18}O_2^{2-}$ peroxide ions. With the increasing of the laser irradiation power, the amount of $(^{18}O^{16}O)^{2-}$ formed on the surface of ^{18}O-labelled Nd_2O_3 increased, suggesting that the diffusion of lattice oxygen species as well as the isotope exchange reaction between $^{16}O^{2-}$ and $^{18}O_2^{2-}$ could be induced by the UV (325 nm) laser irradiation. The photo-induced isotopic exchange between $^{18}O_2$ and lattice oxygen on TiO_2 at room temperature had been previously reported in the literature.[44,45] In addition, the $(^{18}O^{16}O)^{2-}$ peroxide ions can also result from a photo-induced reaction between $^{18}O_2$ and the $^{16}O^{2-}$ species diffused from the bulk phase of the ^{18}O-labelled Nd_2O_3 micro crystals to the surface layer under the experimental conditions.

It is also worth noting that the Raman spectrum of the photooxygenated Nd_2O_3 sample (Fig. S3 in the ESI†) is very similar to that of $Nd_2O_2(O_2)$ (neodymium(III) oxide peroxide) reported by Range *et al.*[36] The latter was prepared from Nd_2O_3 and KO_2 at 1500 °C and 40 kbar. In contrast to such extreme conditions, the present peroxide can be easily generated through a mild photo-induced oxidation of lattice oxygen species with molecular O_2 at room temperature. This process also provides us with a new pathway of activating molecular oxygen on the surface of rare earth oxides by a photochemistry reaction, which may have a potential application in the photo oxidation reaction.

3.2 Effect of basicity of Ln_2O_3 on the formation of peroxide ions

To further elucidate the factors affecting the photo-induced oxidation of the lattice oxygen species in Ln_2O_3 by molecular oxygen, the effects of temperature and laser irradiation power on the formation of peroxide ions over Nd_2O_3, Sm_2O_3 and Gd_2O_3 were investigated. As shown in Fig. 4, the formation and decay of the peroxide bands over Ln_2O_3 was closely related to laser power in conjunction with operating temperatures. After irradiating the samples under O_2 with a 325 nm laser beam of fixed power (2.1 mW) at a temperature between 25 and 600 °C (Fig. 4A), the intensities of the peroxide bands over Nd_2O_3, Sm_2O_3 and Gd_2O_3 were found to peak at about 25, 100 and 200 °C, respectively, indicating that a higher temperature was favorable for the formation of peroxide ions on the Ln_2O_3 with a larger atomic number of Ln. Similarly, for the experiments carried out at a fixed temperature (*e.g.* 25 °C),

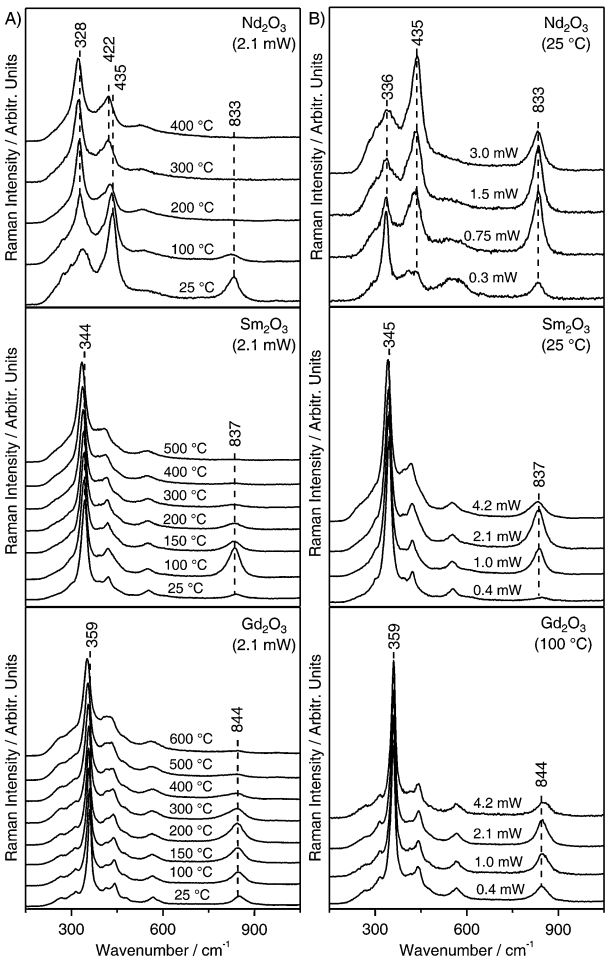

Fig. 4 Effects of temperature and laser irradiation power on the intensity of the peroxide Raman band formed on cubic Ln_2O_3 (Ln = Nd, Sm, Gd). The spectra were recorded after the samples under O_2 were continuously irradiated with (A) a focused 325 nm laser beam of fixed power (2.1 mW) at indicated temperatures, and (B) a focused 325 nm laser beam of indicated powers at fixed temperature (25 or 100 °C) until the intensity of the peroxide band did not increase with increasing laser irradiation time. The temperatures and laser irradiation powers used to record the spectra are indicated in the figures.

higher laser irradiation power was also favored for the reaction between O_2 molecules and the O^{2-} species in Ln_2O_3 with a larger atomic number of Ln (Fig. 4B). These phenomena can be understood in term of the basicity of lanthanide sesquioxides.

As can be seen from the CO_2-TPD profiles of the three Ln_2O_3 samples (Fig. 5), the temperature maximum for the CO_2 desorption peaks decrease in the order $Nd_2O_3 > Sm_2O_3 > Gd_2O_3$. This result clearly indicates that the basicity of the lattice oxygen species in Ln_2O_3 decreases with increasing atomic number of Ln. Since the peroxide ions were generated through a photo-induced oxygenation of lattice oxygen by molecular oxygen in which O^{2-} species in Ln_2O_3 provide the electrons to reduce O_2 molecules, basicity of the O^{2-} in Ln_2O_3 should have a direct impact on the formation of peroxide ions. As a result, a higher energy input (as temperature or laser irradiation power) is required to initiate the reaction between O_2 molecules and the O^{2-} species in Ln_2O_3 with weaker basicity. However, extended irradiation of Nd_2O_3, Sm_2O_3 and Gd_2O_3

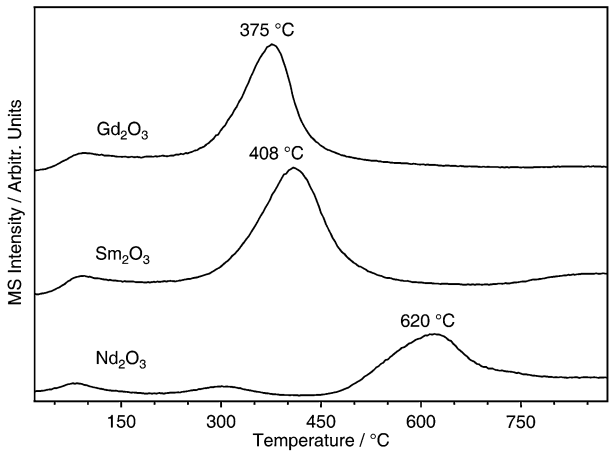

Fig. 5 CO_2-TPD profiles of the cubic Ln_2O_3 (Ln = Nd, Sm, Gd).

samples with a 325 nm laser beam of fixed power (*e.g.* 2.1 mW) at temperatures higher than 25, 100 and 200 °C, respectively (Fig. 4A), or with a laser beam of relatively high power (*e.g.* 3.0 or 4.2 mW, Fig. 4B) may also result in a decrease in the intensity of the peroxide band at 833–844 cm^{-1}, probably due to the photo-induced decomposition of the peroxide ions. It was reported that decomposition of $Nd_2O_2(O_2)$ (as indicated by the disappearance of the ν_{O-O} band at 824 cm^{-1}) was detected after long exposure to 488 nm line of an Ar^+ laser.[46]

3.3 Thermal stability of the peroxide ions on Ln_2O_3

The thermal stability of the peroxide ions on the photooxygenated Ln_2O_3 (Ln = Nd, Sm, Gd) samples were investigated. In the experiments, the Nd_2O_3, Sm_2O_3 and Gd_2O_3 samples under O_2 were first irradiated with a focused 325 nm laser beam at 25, 100 and 200 °C, respectively, to generate the peroxide ions. The photooxygenated sample was then cooled in the dark to 25 °C to record the initial spectrum. After that, the sample was heated in the dark to a specified temperature and maintained there for 10 min. The treated sample was then cooled in the dark to 25 °C to record another spectrum. The same heating–cooling operations were repeated until the peroxide species on the sample were completely decomposed. The corresponding spectra are shown in Fig. 6. As can be seen from the figure, the intensities of the peroxide Raman bands (834–844 cm^{-1}) on the samples remained almost unchanged at temperatures below 300 °C. As the temperature was raised to 400 °C, the intensity of the peroxide Raman bands began to decrease, indicating that the peroxide ions started to decompose at this temperature. The thermal decomposition temperature of the peroxide ions on Ln_2O_3 is very close to that of the $Nd_2O_2(O_2)$ reported by Range *et al.*[47] The latter was found to decompose to cubic Nd_2O_3 and O_2 when the compound was heated under an O_2 or Ar atmosphere to 420 °C. A significant decrease in intensity of the peroxide bands was observed when the temperature of the samples was raised to 450–500 °C. The Raman band of peroxide ions ($\sim$834 cm^{-1}) on Nd_2O_3 vanished after the photooxygenated sample was heated in the dark at 450 °C for 10 min. Comparatively, the thermal stability of the peroxide ions on Sm_2O_3 and Gd_2O_3 is slightly higher than that on Nd_2O_3. Weak O–O stretching vibration bands of the peroxide

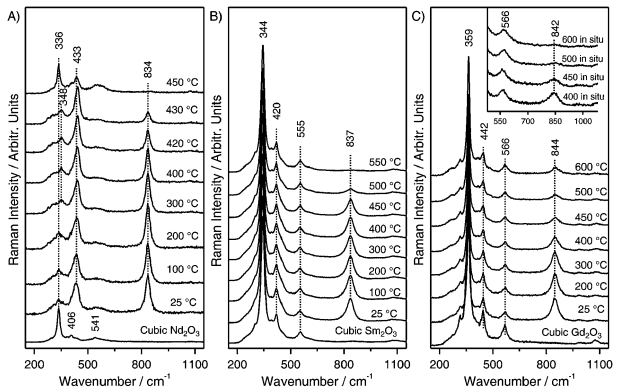

Fig. 6 The decomposition of the peroxide ions on cubic Ln_2O_3 (Ln = Nd, Sm, Gd) at high temperature: (A) Nd_2O_3, (B) Sm_2O_3 and (C) Gd_2O_3. The spectra were recorded at 25 °C after the photo-oxygenated samples were heated in the dark at the indicated temperature for 10 min. For Gd_2O_3, the inset showed the Raman spectra recorded at 400, 450, 500 and 600 °C after the sample was heated in the dark at the temperatures for 10 min. Before the measurements, the Nd_2O_3, Sm_2O_3 and Gd_2O_3 samples under O_2 were irradiated with a focused 325 nm laser beam at 25, 100 and 200 °C, respectively, for 30–90 min until the intensity of the peroxide Raman band did not increase with increasing laser irradiation time. The laser power used to induce the formation of peroxide ions was 0.75 mW for Nd_2O_3, and 2.1 mW for Sm_2O_3 and Gd_2O_3. To minimize the effect of laser irradiation during the spectra recording, all the spectra were recorded with a laser power of 0.3–0.4 mW.

ions (837 and 844 cm^{-1}) on Sm_2O_3 and Gd_2O_3 can still be detected after the photooxygenated samples were heated to 500 and 600 °C, respectively. The stability of the peroxide ions on lanthanide sesquioxides can be understood in term of interactions of the orbitals between Ln_2O_3 and O_2^{2-}. As the atomic numbers of Ln (Ln = Nd, Sm, Gd) increased, the electronegativity (χ) of Ln increased (χ_{Nd} = 1.14, χ_{Sm} = 1.17, χ_{Gd} = 1.20),[48] and the orbitals of Ln_2O_3 to interact with O_2^{2-} are down-shifting in energy, leading to a decrease in the electron back-donation from Ln_2O_3 to the 2π antibonding orbital of O_2^{2-} (as can be seen from Fig. 5, basicity of the three rare earth oxides decreases in the order Nd_2O_3 > Sm_2O_3 > Gd_2O_3), and then an increase in the strength of the O–O bond in O_2^{2-}. Thus, the stability of the peroxide ions on Ln_2O_3 increased with increasing atomic numbers of Ln. This is also in line with the frequency shift of the Raman bands for O–O stretching vibration of the peroxide ions on Nd_2O_3, Sm_2O_3 and Gd_2O_3 (Fig. 1).

Conclusions

In summary, we have demonstrated that an O_2 molecule can be selectively transformed to O_2^{2-} ion by a photo-induced reaction with the lattice oxygen species of lanthanide sesquioxides. Under the excitation of 325 nm UV light, the reaction between O_2 and the O^{2-} on the surfaces of Nd_2O_3, Sm_2O_3 and Gd_2O_3 can even take place at room temperature. This process provides us with a new pathway of activating molecular oxygen on the surface of lanthanide oxides under mild conditions. The results of the investigation also give us new insight into the mechanism of O_2 activation on the surface of metal oxides with stable cationic valance. The peroxide ion has been suggested as the active oxygen species in many catalytic oxidation reactions.[49–53] The peroxide species formed by photo-induced reaction between O_2 and O^{2-} should have the same chemical properties as those produced in thermal processes and possess a potential application in photocatalytic reactions. Further research is in progress to investigate its catalytic functions.

Acknowledgements

We thank the National Basic Research Program of China (2010CB732303), the National Natural Science Foundation of China (21173173, 21033006, and 20923004) and the Program for Changjiang Scholars and Innovative Research Team in University (IRT1036) for financial support.

Notes and references

1 G. Centi, F. Cavani and F. Trifirò, *Selective oxidation by heterogeneous catalysis*, Kluwer Academic/Plenum, New York, 2001.
2 J. H. Tong, Z. Li and C. G. Xia, *Prog. Chem.*, 2005, **17**, 96.
3 A. Bielański and J. Haber, *Oxygen in Catalysis*, Marcel Dekker, New York, 1991.
4 J. Haber, *Selective Oxidation – Heterogeneous*, *Encyclopedia of Catalysis*, John Wiley & Sons Inc., 2002.
5 R. A. van Santen and M. Neurock, *Molecular Heterogeneous Catalysis: A Conceptual and Computational Approach*, Wiley-VCH, Weinheim, 2006.
6 G. Ertl, H. Knözinger and J. Weitkamp, *Handbook of Heterogeneous Catalysis*, Wiley-VCH, Weinheim, 1997.
7 G. A. Martin, S. Bernal, V. Perrichon and C. Mirodatos, *Catal. Today*, 1992, **13**, 487.
8 C. T. Au, K. D. Chen and C. F. Ng, *Appl. Catal., A*, 1998, **170**, 81.
9 O. V. Buyevskaya, D. Wolf and M. Baerns, *Catal. Today*, 2000, **62**, 91.
10 S. F. Håkonsen and A. Holmen, *Oxidative Dehydrogenation of Alkanes*, in *Handbook of Heterogeneous Catalysis*, Wiley-VCH Verlag GmbH & Co KGaA, 2008, p. 3384.
11 H. L. Wan, X. P. Zhou, W. Z. Weng, R. Q. Long, Z. S. Chao, W. D. Zhang, M. S. Chen, J. Z. Luo and S. Q. Zhou, *Catal. Today*, 1999, **51**, 161.
12 A. G. Dedov, A. S. Loktev, I. I. Moiseev, A. Aboukais, J. F. Lamonier and I. N. Filimonov, *Appl. Catal., A*, 2003, **245**, 209.
13 L. Olivier, S. Haag, H. Pennemann, C. Hofmann, C. Mirodatos and A. C. van Veen, *Catal. Today*, 2008, **137**, 80.
14 J. H. Lunsford, *Catal. Today*, 1990, **6**, 235.
15 C. H. Lin, K. D. Campbell, J. X. Wang and J. H. Lunsford, *J. Phys. Chem.*, 1986, **90**, 534.
16 J. H. Lunsford, *Angew. Chem., Int. Ed. Engl.*, 1995, **34**, 970.
17 G. J. Hutchings, J. R. Woodhouse and M. S. Scurrell, *J. Chem. Soc., Faraday Trans. 1*, 1989, **85**, 2507.
18 Z. Kalenik and E. E. Wolf, *Catal. Today*, 1992, **13**, 255.
19 S. J. Huang, A. B. Walters and M. A. Vannice, *J. Catal.*, 2000, **192**, 29.
20 S. Lacombe, H. Zanthoff and C. Mirodatos, *J. Catal.*, 1995, **155**, 106.
21 E. S. R. Winter, *J. Chem. Soc. A*, 1969, 1832.
22 M. S. Palmer, M. Neurock and M. M. Olken, *J. Phys. Chem. B*, 2002, **106**, 6543.
23 G. Mestl, H. Knözinger and J. H. Lunsford, *Bunsen-Ges. Phys. Chem., Ber.*, 1993, **97**, 319.
24 Y. D. Liu, H. B. Zhang, G. D. Lin, Y. Y. Liao and K. R. Tsai, *J. Chem. Soc., Chem. Commun.*, 1994, 1871.
25 W. Z. Weng, H. L. Wan, J. M. Li and Z. X. Cao, *Angew. Chem., Int. Ed.*, 2004, **43**, 975.
26 M. W. Shafer and R. J. Roy, *J. Am. Ceram. Soc.*, 1959, **42**, 563.
27 J. Tong and L. J. Eyring, *J. Alloys Compd.*, 1995, **225**, 139.
28 W. Z. Weng, X. Q. Pei, J. M. Li, C. R. Luo, Y. Liu, H. Q. Lin, C. J. Huang and H. L. Wan, *Catal. Today*, 2006, **117**, 53.
29 W. B. White and V. G. Keramidas, *Spectrochim. Acta, Part A*, 1972, **28**, 501.

30 N. Dilawar, S. Mehrotra, D. Varandani, B. V. Kumaraswamy, S. K. Haldar and A. K. Bandyopadhyay, *Mater. Charact.*, 2008, **59**, 462.
31 A. Ubaldini and M. M. Carnasciali, *J. Alloys Compd.*, 2008, **454**, 374.
32 Y. Repelin, C. Proust, E. Husson and J. M. Beny, *J. Solid State Chem.*, 1995, **118**, 163.
33 G. Schaack and J. A. Koningstein, *J. Opt. Soc. Am.*, 1970, **60**, 1110.
34 L. A. Tucker, F. J. Carney, P. McMillan, S. H. Lin and L. Eyring, *Appl. Spectrosc.*, 1984, **38**, 857.
35 H. H. Eysel and S. Thym, *Z. Anorg. Allg. Chem.*, 1975, **411**, 97.
36 A. M. Heyns and K. J. Range, *J. Raman Spectrosc.*, 1994, **25**, 855.
37 W. Hesse, M. Jansen and W. Schnick, *Prog. Solid State Chem.*, 1989, **19**, 47.
38 V. A. Shvets, V. M. Vorotyntsev and V. B. Kazanskii, *Kinet. Katal.*, 1969, **10**, 356.
39 V. B. Kazansky, *Kinet. Katal.*, 1977, **18**, 43.
40 A. Bielański and J. Harber, *Catal. Rev. Sci. Eng.*, 1979, **19**, 1.
41 M. S. Palmer, M. Neurock and M. M. Olken, *J. Am. Chem. Soc.*, 2002, **124**, 8452.
42 N. X. Lu, G. Fu, X. Xu and H. L. Wan, *J. Chem. Phys.*, 2008, **128**, 034702.
43 J. H. Lunsford, X. Yang, K. Haller, J. Laane, G. Mestl and H. Knozinge, *J. Phys. Chem.*, 1993, **97**, 13810.
44 H. Courbon, M. Formenti and P. Pichat, *J. Phys. Chem.*, 1977, **81**, 550.
45 S. Sato, T. Kadowaki and K. Yamaguti, *J. Phys. Chem.*, 1984, **88**, 2930.
46 A. M. Heyns and K. J. Range, *J. Alloys Compd.*, 1991, **176**, L17.
47 K. J. Range, M. Stadler, F. Rau and U. Klement, *Angew. Chem., Int. Ed. Engl.*, 1987, **26**, 1174.
48 J. A. Dean, *Lange's Handbook of Chemistry*, McGraw-Hill Book Company, New York, 15th edn, 1999, section 4, 4.29.
49 Y. Wang, K. Otsuka and K. Ebitani, *Catal. Lett.*, 1995, **35**, 259.
50 K. C. C. Kharas and J. H. Lunsford, *J. Am. Chem. Soc.*, 1989, **111**, 2336.
51 H. Yamashita, Y. Machida and A. Tomita, *Appl. Catal., A*, 1991, **79**, 203.
52 G. Mestl, M. P. Rosynek and J. H. Lunsford, *J. Phys. Chem. B*, 1998, **102**, 154.
53 H. X. Dai, C. F. Ng and C. T. Au, *Appl. Catal., A*, 2000, **202**, 1.

